Final Technical Report:

Real Time Trajectory Planning for Groups of Unmanned Vehicles

Farbod Fahimi
Center of Nonlinear Dynamics and Control (CENDAC)
Villanova University
Villanova, PA 19085
Email: farbod.fahimi@villanova.edu

August 22, 2005

Abstract

Feedback control laws for controlling multiple unmanned surface vehilces in arbitrary formations are proposed. The presented formation control method uses only local sensor-based information. The method of input-output linearization has been used to exponentially stabilize the relative distance and orientation of neighboring vehicles with a three-degree-of-freedom dynamic model. It is shown that the internal dynamics of the system is also stable. The use of these control laws is demonstrated by computer simulations. These controllers can be utilized to control an arbitrarily large number of unmanned vehicles moving in very general formations.

1 Introduction

During the last several years, researchers have investigated the formation control problem for different type of vehicles, including indoor mobile robots, outdoor ground vehicles, aerial vehicles, and underwater and surface vehicles. The robotic research literature are richer in this regard. Researchers of this field have used kinematic models of holonomic robots and proposed feedback control laws to control the group of robots such that they capture/enclose a target by making troop formations [1]. In this method, the robots do not maintain a predefined formation during the motion. They change their formation autonomously to surround a target. Other researchers in the robotics field have implemented a set of elementary behaviors (obstacle avoidance and formation maintaining behaviors) to control team formations. They have designed a fuzzy controller based on holonomic kinematic models for each behavior. The overall response of the robot was the weighted superposition of each behavior [2].

Also, investigators have considered three sets of geometric parameters to describe the configuration of a robot team. One set defines the gross position of a lead robot, a second set describes the relative positions of the robots, and a third set determines the local relations of the neighboring robots. They have used a nonholonomic kinematic model for the robots and designed nonlinear feedback controllers [3].

Researchers have recently designed decentralized feedback laws for a formation of unmanned aerial vehicles (UAVs). They have treated the dynamic model of the formation structure as an interconnected system with overlapping subsystems. They have designed a static state feedback controller for each subsystem based on their perturbed nominal dynamics [4].

Some researchers have considered the formation control problem for unmanned underwater vehicles (UUVs). They have presented a biologically inspired, decentralized methodology for moving a loose formation of UUVs with the goal of minimizing outside guidance [5]. Others have proposed an integrated acoustic navigation system and coordination control maneuver for a formation of three UUVs and one surface craft [6].

Naval researchers have investigated decentralized formation control schemes for a fleet of vessels with a small amount of intervessel communication [7]. In their approach, each vessel maintains its position in the formation relative to a Formation Reference Point, which follows a predefined path. They have constructed an individual parametrized path for each vessel so that when the parametrization variables are synchronized, the vessels are in formation.

In the current paper, the problem of control and coordination for many unmanned surface vehicles moving in formation is investigated. The overall motion plan for a single unmanned lead vehicle, which can be a virtual vehicle, is assumed. The dynamic models of the vehicles are considered for designing the controllers. It consists of the surge, sway, and yaw degrees of freedom. It is assumed that two independent actuators drive the vehicle.

Two nonlinear decentralized schemes are designed for feedback control within a formation. In the first scheme, one vehicle controls its relative distance and orientation with respect to a neighboring vehicle. In the second scheme, a vehicle maintains its position in the formation by maintaining specified distances from two neighboring vehicles, or from one vehicle and an obstacle. The idea of controlling relative distances is adapted from robotics research [3].

The proposed control schemes use only local sensor-based information. Feedback linearization method is used and it is shown that the relative distances and orientations of the vehicles are exponentially stabilized. The stability of zero dynamics of the system is also discussed. These control laws have the advantage of providing easily computable, real-time feedback control, with provable performance for the entire system. Numerical simulations are presented to demonstrate the efficiency of these techniques.

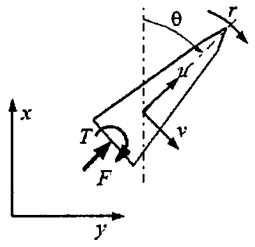

Figure 1: A 3 DOF Dynamic Model of a Vehicle

2 Dynamics of a Surface Vehicle

This sections presents the dynamic model of a vehicle, shown in Fig. 1. Three degrees of freedom, surge, sway, and yaw, are assumed for each vehicle. u, v, and r, denote the speeds of these DOFs in local coordinate system respectively. A propeller and a rudder, or two independent thrusters can provide the driving force and steering torque for the system. The force and torque are denoted by F and T respectively. Note that in each case only two independent actuations are available for each 3 DOF vehicle. Therefore the vehicle is an underactuated dynamic system, and the stability of its zero dynamics becomes a concern.

It has been shown that with the assumptions of constant inertia, an elliptical vehicle body, negligible higher order damping terms, and simplification of the hydrodynamics, the following equations describe the dynamics of the vehicle in the local coordinate system [8].

$$\begin{aligned} m_{11}\dot{u} - m_{22}vr + d_{11}u &= F \\ m_{22}\dot{v} + m_{11}ur + d_{22}v &= 0 \\ m_{33}\dot{r} + (m_{22} - m_{11})uv + d_{33}r &= T \end{aligned} \tag{1}$$

m_{ij}'s are the mass and moment of inertia of the vehicles including the hyrodynamic added mass and moment of inertia, and d_{ij}'s are the damping coefficients. One can use the kinematic relations between the speeds in local and global coordinate systems and obtain the dynamic equations in terms of the global coordinates as:

$$\begin{aligned} \ddot{x} &= \tfrac{1}{m_{11}}\,(f_x + F\ \mathrm{c}\theta) \\ \ddot{y} &= \tfrac{1}{m_{22}}\,(f_y + F\ \mathrm{s}\theta) \\ \ddot{\theta} &= \tfrac{1}{m_{33}}\,(f_\theta + T) \end{aligned} \tag{2}$$

where c = cos, s = sin, and,

$$\begin{aligned} f_x &= m_r d_{22} v\ \mathrm{s}\theta - d_{11}u\ \mathrm{c}\theta + \dot{\theta}(v\ \mathrm{c}\theta - m_r u\ \mathrm{s}\theta)m_d \\ f_y &= -m_r d_{22} v\ \mathrm{c}\theta - d_{11}u\ \mathrm{s}\theta + \dot{\theta}(v\ \mathrm{s}\theta + m_r u\ \mathrm{c}\theta)m_d \\ f_\theta &= -m_d uv - d_{33}\dot{\theta} \end{aligned} \tag{3}$$

and,

$$m_d = m_{22} - m_{11}$$
$$m_r = \frac{m_{11}}{m_{22}}$$

Equations (2) and (3) describe the dynamics of the vehicles in terms of the global coordinate components.

3 Formation Control Schemes

The bulk motion of the group of vehciles can be characterized by trajectory planning and obstacle avoidance algorithms, for example, the method of artificial potential fields [9]. It is assumed that a hypothetical vehicle as a group leader adapts the bulk motion of the group as its planned trajectory and other vehicles of the group follow either the hypothetical group leader or their neighboring vehicles. Therefore, our attention is focused on controlling the internal geometry of the formation. Two types of feedback controllers are designed for controlling the internal geometry.

The first feedback controller is called the $l - \psi$ controller. It controls the relative distance and view angle of a vehicle with respect to a neighboring vehicle. This situation is applicable to all formations in which each vehicle sees one neighbor. Thus it can be used for vehicles marching in a single file or at an edge of the formation geometry.

Note that the $l - \psi$ controller alone can not define a general formation. When a vehicle is constrained by more than one neighbor (or obstacle) in the formation, a second feedback controller is needed to control the distances of the vehicle from two neighboring vehicles, or from one vehicle and an obstacle. This controller is called the $l - l$ controller.

These two local controllers are necessary to define a general formation. Usually the vehicles at an edge of the formation geometry control their distance with their immediate front vehicle using the $l - \psi$ controller. The other vehicles control their distances to their immediate front and side vehicles using the $l - l$ controller. This is necessary so that a vehicle can also avoid its side vehicle. Detailed examples are presented in the simulation section of this paper.

3.1 Design of the $l - \psi$ controller

In Fig. 2, a system of two neighboring vehicles in the formation is shown. The vehicles are separated by a distance l_{12} between the center of mass of vehicle 1 and an arbitrary point, p, on vehicle 2. The arbitrary point has a distance d with the center of mass. Note that the vehicles are not physically coupled in any way. A feedback control law for control inputs F_2 and T_2 must be determined to control vehicle 2 such that the desired distance l_{12}^d and view angle ψ_{12}^d to vehicle 1 are maintained. Therefore the outputs of the control system are: $[l_{12}, \psi_{12}]$. The state variables that define the dynamics of vehicle 2 are: $[x_2, y_2, \theta_2]$. The

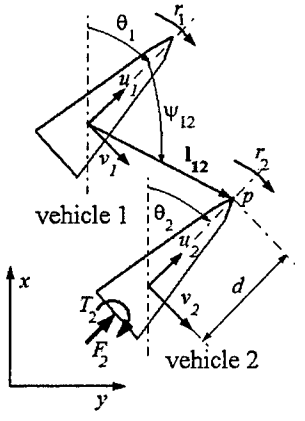

Figure 2: $l - \psi$ Control Configuration

state variable-output relations of this control system are obtained by writing the kinematics equation for $l - \psi$ configuration.

Acceleration of point p on vehicle 2 can be written in two ways, once with respect to center of mass of vehicle 1 and once with respect to that of vehicle 2. The resulting equations are solved for the highest derivatives of the outputs l_{12} and ψ_{12} to obtain state variable-output relations.

$$\begin{aligned} \ddot{l}_{12} = (\ddot{y}_2 - \ddot{y}_1)\ \mathrm{s}\alpha_0 + (\ddot{x}_2 - \ddot{x}_1)\ \mathrm{c}\alpha_0 + d\ddot{\theta}_2\ \mathrm{s}\gamma_1 \\ -d\dot{\theta}_2^2\ \mathrm{c}\gamma_1 + l_{12}\dot{\alpha}_0^2 \end{aligned} \tag{4}$$

$$\begin{aligned} \ddot{\psi}_{12} = \tfrac{1}{l_{12}}[(\ddot{y}_2 - \ddot{y}_1)\ \mathrm{c}\alpha_0 - (\ddot{x}_2 - \ddot{x}_1)\ \mathrm{s}\alpha_0 + d\ddot{\theta}_2\ \mathrm{c}\gamma_1 \\ +d\dot{\theta}_2^2\ \mathrm{s}\gamma_1 - 2\dot{l}_{12}\dot{\alpha}_0 - l_{12}\ddot{\theta}_1] \end{aligned} \tag{5}$$

where

$$\begin{aligned} \alpha_0 &= \theta_1 + \psi_{12} \\ \gamma_1 &= \theta_1 + \psi_{12} - \theta_2 \end{aligned}$$

The goal is finding a control law for the two inputs $[F_2, T_2]$ to stabilize the outputs. Therefore, the input-output equations are first obtained by writing the dynamic equations (2) for vehicle 2 and substituting the results into the kinematics equations (4) and (5).

$$\ddot{l}_{12} = \left[f_l + \tfrac{1}{m_{11}} F_2\ \mathrm{c}\gamma_1 + \tfrac{1}{m_{33}} T_2 d\ \mathrm{s}\gamma_1\right] \tag{6}$$

$$\ddot{\psi}_{12} = \tfrac{1}{l_{12}}\left[f_\psi - \tfrac{1}{m_{11}} F_2\ \mathrm{s}\gamma_1 + \tfrac{1}{m_{33}} T_2 d\ \mathrm{c}\gamma_1\right] \tag{7}$$

where

$$f_l = \frac{1}{m_{11}}(f_x \ c\alpha_0 + f_y \ s\alpha_0) + \frac{1}{m_{33}} f_\theta d \ s\gamma_1 - \ddot{x}_1 \ c\alpha_0 - \ddot{y}_1 \ s\alpha_0$$
$$-d\dot{\theta}_2^2 \ c\gamma_1 + l_{12}\dot{\alpha}_0^2$$
$$f_\psi = \frac{1}{m_{11}}(-f_x \ s\alpha_0 + f_y \ c\alpha_0) + \frac{1}{m_{33}} f_\theta d \ c\gamma_1 + \ddot{x}_1 \ s\alpha_0 - \ddot{y}_1 \ c\alpha_0$$
$$+d\dot{\theta}_2^2 \ s\gamma_1 - 2\dot{l}_{12}\dot{\alpha}_0 - l_{12}\ddot{\theta}_1$$

Input-output linearization is used to design a controller based on the input-output equations (6) and (7). In this method, an asymptotically stable second order error dynamics is assumed ($\lambda_i > 0$):

$$\ddot{e}_i + 2\lambda_i \dot{e}_i + \lambda_i^2 e_i = 0 \qquad i = 1, 2 \tag{8}$$

where e_1 and e_2 are the output errors defined as:

$$e_1 = l_{12} - l_{12}^d \qquad e_2 = \psi_{12} - \psi_{12}^d \tag{9}$$

Now, the control laws are derived by combining Eqns. (8) and (9), substituting the results into input-output equations (6) and (7), and solving for inputs F_2 and T_2.

$$F_2 = m_{11}[(\ddot{l}_{12}^d - 2\lambda_1 \dot{e}_1 - \lambda_1^2 e_1 - f_l) \ c\gamma_1$$
$$- (l_{12}(\ddot{\psi}_{12}^d - 2\lambda_2 \dot{e}_2 - \lambda_2^2 e_2) - f_\psi) \ s\gamma_1] \tag{10}$$

$$T_2 = \frac{m_{33}}{d}[(\ddot{l}_{12}^d - 2\lambda_1 \dot{e}_1 - \lambda_1^2 e_1 - f_l) \ s\gamma_1$$
$$- (l_{12}(\ddot{\psi}_{12}^d - 2\lambda_2 \dot{e}_2 - \lambda_2^2 e_2) - f_\psi) \ c\gamma_1] \tag{11}$$

The distance l_{12} and view angle ψ_{12} in the $l - \psi$ configuration shown in Fig. 2 asymptotically converge to their corresponding desired values, because the control laws (10) and (11) guarantee that errors vanish as time approaches infinity. But θ_2, the orientation of vehicle 2, is not directly controlled. The dynamics of this degree of freedom when others have been stabilized is referred to as the zero dynamics of the system and its stability has to be investigated separately.

3.2 Zero dynamics stability for the $l - \psi$ controller

In this section, the stability of the zero dynamics is proven by considering the relation between the controlled outputs and the orientation of vehicle 2. This relation is obtained by the velocity analysis of the $l - \psi$ configuration shown in Fig. 2 as:

$$\dot{l}_{12} = [(\dot{y}_2 - \dot{y}_1) \ s\alpha_0 + (\dot{x}_2 - \dot{x}_1) \ c\alpha_0 + d\dot{\theta}_2 \ s\gamma_1] \tag{12}$$
$$\dot{\psi}_{12} = \frac{1}{l_{12}}[(\dot{y}_2 - \dot{y}_1) \ c\alpha_0 - (\dot{x}_2 - \dot{x}_1) \ s\alpha_0 + d\dot{\theta}_2 \ c\gamma_1$$
$$-l_{12}\dot{\theta}_1] \tag{13}$$

Note that $l_{12} = l_{12}^d$, $\psi_{12} = \psi_{12}^d$, $\dot{l}_{12} = 0$, and $\dot{\psi}_{12} = 0$, after the controlled outputs have reached the steady state. These conditions are applied to Eqns. (12) and (13) and the results are solved for $\dot{\theta}_2$:

$$\dot{\theta}_2 = \frac{1}{d}\left(-v_2 + \dot{y}_1 \ \mathrm{c}\theta_2 - \dot{x}_1 \ \mathrm{s}\theta_2 + l_{12}^d \dot{\theta}_1 \ \mathrm{c}\gamma_1\right) \tag{14}$$

where $v_2 = \dot{y}_2 \ \mathrm{c}\theta_2 - \dot{x}_2 \ \mathrm{s}\theta_2$ is the lateral velocity of vehicle 2. Equation (14) describes the zero dynamics of the $l - \psi$ controller. This equation is used to analyze the stability of zero dynamics in cases of circular and linear motions.

3.2.1 Circular motion

First, the stability of θ_2 is analyzed when vehicle 1 has a circular motion with constant linear speed $s_1 = (u_1^2 + v_1^2)^{0.5}$. For a circular motion, the orientation of vehicle 1 is $\theta_1 = \omega t + \theta_{10}$, where θ_{10} is its initial orientation 1. The velocity components of the motion of vehicle 1 become:

$$\dot{x}_1 = s_1 \ \mathrm{c}\theta_1 \qquad \dot{y} = s_1 \ \mathrm{s}\theta_1 \tag{15}$$

Equation (15) is substituted in Eqn. (14) to obtain:

$$\dot{\theta}_2 = \tfrac{1}{d}(-v_2 + s_1 \ \mathrm{s}(\theta_1 - \theta_2) + l_{12}^d \omega \ \mathrm{c}(\theta_1 - \theta_2 + \psi_{12}^d)) \tag{16}$$

This can be further manipulated to obtain the simpler form:

$$\dot{\theta}_2 = \frac{1}{d}\left(\beta_1 \ \mathrm{c}(\theta_1 - \theta_2 + \beta_2) - v_2\right) \tag{17}$$

where β_1 and β_2 are constants.

$$\beta_1 = \sqrt{(s_1 - l_{12}^d \omega \ \mathrm{s}\psi_{12}^d)^2 + (l_{12}^d \omega \ \mathrm{c}\psi_{12}^d)^2}$$
$$\beta_2 = \arctan\left(\tfrac{s_1 - l_{12}^d \omega \ \mathrm{s}\psi_{12}^d}{l_{12}^d \omega \ \mathrm{c}\psi_{12}^d}\right)$$

A change of variable to $\delta_{12} = \theta_1 - \theta_2$ is made and the following differential equation is obtained:

$$\dot{\delta}_{12} = \frac{1}{d}\left(v_2 + \omega d - \beta_1 \ \mathrm{c}(\delta_{12} - \beta_2)\right) \tag{18}$$

Note that vehicle 1 is moving on a circle and vehicle 2 is maintaining a constant distance with vehicle 1. Therefore, vehicle 2 is also moving on a circle. By observing the dynamic equations (1), one can conclude that for such a motion v_2 is constant. Therefore all parameters in Eqn. (18) are constants, and one can easily show the asymptotic stability of the following fixed equilibrium point.

$$\delta_{12}^e = \arccos\left(\frac{\omega d + v_2}{\beta_1 d}\right) + \beta_2 \tag{19}$$

Thus the motion of vehicle 2 will locally converge to the equilibrium trajectory:

$$\theta_2^e = \theta_1 - \delta_{12}^e \tag{20}$$

3.2.2 Linear motion

The stability of zero dynamics is also analyzed when vehicle 1 moves on a straight line. In this case, the velocity components of vehicle 1 become:

$$\dot{x}_1 = u_1 \, \mathrm{c}\theta_{10} \qquad \dot{y}_1 = u_1 \, \mathrm{s}\theta_{10} \qquad \dot{\theta}_1 = 0 \tag{21}$$

where u_1 is the linear velocity and θ_{10} is the orientation of vehicle 1. Substituting Eqns. (21) into Eqn. (14) and simplifying results in:

$$\dot{\theta}_2 = \frac{1}{d}\left(-v_2 + u_1 \, \mathrm{s}(\theta_{10} - \theta_2)\right) \tag{22}$$

One can obtain the following differential equation with a change of variable to $\delta_{12} = \theta_{10} - \theta_2$:

$$\dot{\delta}_{12} = \frac{1}{d}(v_2 - u_1 \, \mathrm{s}\delta_{12}) \tag{23}$$

Since vehicle 1 is moving on a line and vehicle 2 is maintaining a constant distance with vehicle 1, vehicle 2 is also moving on a line. If the dynamic equations (1) are simplified with this assumption, it can be shown that for a linear motion v_2 is zero. Thus, all the parameters in Eqn. (18) are constant, and linearization of (18) can easily show the asymptotic stability of the following constant equilibrium point.

$$\delta_{12}^e = 0 \tag{24}$$

Thus the motion of the vehicles will locally converge to the equilibrium trajectory:

$$\theta_2^e = \theta_{10} \tag{25}$$

3.3 Design of the $l - l$ controller

In Fig. 3, a system of three vehicles is shown. A controller must be designed to stabilize the distance of vehicle 3 from the two neighboring vehicles. Distances are measured from the centers of mass of vehicles 1 and 2 to an arbitrary point on vehicle 3, which is offset by d from its center of mass. The feedback controller inputs are the driving force and the steering torque of vehicle 3, F_3 and T_3. The desired distances l_{13}^d and l_{23}^d to vehicles 1 and 2, respectively, are to be maintained. Thus the outputs of the control system are: $[l_{13}, l_{23}]$. The state variables that define the dynamics of vehicle 3 are: $[x_3, y_3, \theta_3]$. The state variable-output relations of this control system are obtained by writing the kinematics equation for the $l - l$ configuration.

The same procedure of writing the acceleration kinematic equations for point p that was introduced in $l - \psi$ control can be repeated here. These kinematic equations can be solved for the second-order derivative of l_{13} and l_{23}. This gives

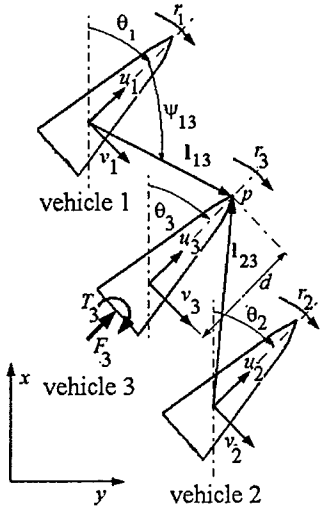

Figure 3: $l-l$ Control Configuration

the following state variable-output equations.

$$\begin{aligned}\ddot{l}_{13} = (\ddot{y}_3 - \ddot{y}_1)\ \mathrm{s}\alpha_1 + (\ddot{x}_3 - \ddot{x}_1)\ \mathrm{c}\alpha_1 + d\ddot{\theta}_3\ \mathrm{s}\gamma_2 \\ -d\dot{\theta}_3^2\ \mathrm{c}\gamma_2 + l_{13}\dot{\alpha}_1^2 \qquad (26)\end{aligned}$$

$$\begin{aligned}\ddot{l}_{23} = (\ddot{y}_3 - \ddot{y}_2)\ \mathrm{s}\alpha_2 + (\ddot{x}_3 - \ddot{x}_2)\ \mathrm{c}\alpha_2 + d\ddot{\theta}_3\ \mathrm{s}\gamma_3 \\ -d\dot{\theta}_3^2\ \mathrm{c}\gamma_3 + l_{23}\dot{\alpha}_2^2 \qquad (27)\end{aligned}$$

where

$$\begin{aligned}\alpha_1 &= \theta_1 + \psi_{13} \qquad \gamma_2 = \theta_1 + \psi_{13} - \theta_3 \\ \alpha_2 &= \theta_2 + \psi_{23} \qquad \gamma_3 = \theta_2 + \psi_{23} - \theta_3\end{aligned}$$

Since the goal is finding a control law for the two inputs $[F_3, T_3]$ to stabilize the outputs, the input-output equations are needed. These equations are obtained by writing the dynamic equations (2) for vehicle 3 and substituting the results into the kinematics equations (26) and (27).

$$\ddot{l}_{13} = f_1 + \tfrac{1}{m_{11}} F_3\ \mathrm{c}\gamma_2 + \tfrac{1}{m_{33}} T_3 d\ \mathrm{s}\gamma_2 \qquad (28)$$

$$\ddot{l}_{23} = f_2 + \tfrac{1}{m_{11}} F_3\ \mathrm{c}\gamma_3 + \tfrac{1}{m_{33}} T_3 d\ \mathrm{s}\gamma_3 \qquad (29)$$

where

$$f_1 = \frac{1}{m_{11}}(f_x \ \mathrm{c}\alpha_1 + f_y \ \mathrm{s}\alpha_1) + \frac{1}{m_{33}} f_\theta d \ \mathrm{s}\gamma_2 - \ddot{x}_1 \ \mathrm{c}\alpha_1 - \ddot{y}_1 \ \mathrm{s}\alpha_1 \\ -d\dot{\theta}_3^2 \ \mathrm{c}\gamma_2 + l_{13}\dot{\alpha}_1^2$$

$$f_2 = \frac{1}{m_{11}} f_x \ \mathrm{c}\alpha_2 + f_y \ \mathrm{s}\alpha_2 + \frac{1}{m_{33}} f_\theta d \ \mathrm{s}\gamma_3 - \ddot{x}_2 \ \mathrm{c}\alpha_2 - \ddot{y}_2 \ \mathrm{s}\alpha_2 \\ -d\dot{\theta}_3^2 \ \mathrm{c}\gamma_3 + l_{23}\dot{\alpha}_2^2$$

A controller is designed for input-output equations (28) and (29) via input-output linearization. The output errors are defined as

$$e_1 = l_{13} - l_{13}^d \qquad e_2 = l_{23} - l_{23}^d \tag{30}$$

and an asymptotically stable second order error dynamics is assumed ($\lambda_i > 0$):

$$\ddot{e}_i + 2\lambda_i \dot{e}_i + \lambda_i^2 e_i = 0 \qquad i = 1, 2 \tag{31}$$

Now, the control laws are derived by combining Eqns. (30) and (31), substituting the results into input-output equations (28) and (29), and solving for inputs F_3 and T_3.

$$F_3 = \frac{m_{11}}{\mathrm{s}(\alpha_2 - \alpha_1)}[(\ddot{l}_{13}^d - 2\lambda_1 \dot{e}_1 - \lambda_1^2 e_1 - f_1) \ \mathrm{s}\gamma_3 \\ - (\ddot{l}_{23}^d - 2\lambda_2 \dot{e}_2 - \lambda_2^2 e_2 - f_2) \ \mathrm{s}\gamma_2] \tag{32}$$

$$T_3 = \frac{m_{33}}{d \ \mathrm{s}(\alpha_2 - \alpha_1)}[-(\ddot{l}_{13}^d - 2\lambda_1 \dot{e}_1 - \lambda_1^2 e_1 - f_1) \ \mathrm{c}\gamma_3 \\ + (\ddot{l}_{23}^d - 2\lambda_2 \dot{e}_2 - \lambda_2^2 e_2 - f_2) \ \mathrm{c}\gamma_2] \tag{33}$$

The control laws (32) and (33) guarantee that the distance l_{13} and l_{23} in the $l-l$ configuration shown in Fig. 3 asymptotically converge to their corresponding desired values. But the orientation of vehicle 3, θ_3, is not directly controlled and its response after the outputs have converged (the zero dynamics of the system) has to be investigated.

3.4 Zero dynamics stability for the $l - l$ controller

In this section, the stability of the zero dynamics is proven. The velocity analysis of vehicles 1 and 3 in $l - l$ configuration results in the following kinematic equations, which describe the relation between the controlled output l_{13}, the view angle ψ_{13}, and the orientation of vehicle 3.

$$\dot{l}_{13} = [(\dot{y}_3 - \dot{y}_1) \ \mathrm{s}\alpha_1 + (\dot{x}_3 - \dot{x}_1) \ \mathrm{c}\alpha_1 + d\dot{\theta}_3 \ \mathrm{s}\gamma_2] \tag{34}$$

$$\dot{\psi}_{13} = \frac{1}{l_{13}}[(\dot{y}_3 - \dot{y}_1) \ \mathrm{c}\alpha_1 - (\dot{x}_3 - \dot{x}_1) \ \mathrm{s}\alpha_1 + d\dot{\theta}_3 \ \mathrm{c}\gamma_2 \\ - l_{13}\dot{\theta}_1] \tag{35}$$

After the controlled outputs have reached the equilibrium, $l_{13} = l_{13}^d$, $l_{23} = l_{23}^d$, $\dot{l}_{13} = 0$, and $\dot{l}_{23} = 0$. Note that these equilibrium conditions also imply that ψ_{13} becomes stabilized at some value ψ_{13}^e and $\dot{\psi}_{13} = 0$. These conditions are applied to (34) and (35) and the results are solved for $\dot{\theta}_3$:

$$\dot{\theta}_3 = \frac{1}{d}\left(-v_3 + \dot{y}_1\ \mathrm{c}\theta_3 - \dot{x}_1\ \mathrm{s}\theta_3 + l_{13}^d\dot{\theta}_1\ \mathrm{c}\gamma_2\right) \tag{36}$$

where $v_3 = \dot{y}_3\ \mathrm{c}\theta_3 - \dot{x}_3\ \mathrm{s}\theta_3$ is the lateral velocity of vehicle 3. Equation (36) describes the zero dynamics of the $l-l$ control system. This equation is very similar to Eqn. (14) in nature. Thus the procedure discussed about the stability of $l-\psi$ controller can be repeated. It can be shown that for a circular motion of the group of three vehicles with constant speed, where $\theta_1 = \omega t + \theta_{10}$ and $\dot{\theta}_1 = \omega$, the orientation of vehicle 3 converges to the following equilibrium trajectory:

$$\theta_3^e = \theta_1 - \delta_{13}^e \tag{37}$$

where

$$\delta_{13}^e = \arccos\left(\frac{\omega d + v_3}{\beta_3 d}\right) + \beta_4 \tag{38}$$

and

$$\beta_3 = \sqrt{(s_1 - l_{13}^d\omega\ \mathrm{s}\psi_{13}^e)^2 + (l_{13}^d\omega\ \mathrm{c}\psi_{13}^e)^2}$$
$$\beta_4 = \arctan\left(\frac{s_1 - l_{13}^d\omega\ \mathrm{s}\psi_{13}^e}{l_{13}^d\omega\ \mathrm{c}\psi_{13}^e}\right)$$

Note that v_3 is constant for a circular motion, and s_1 is the constant linear velocity of vehicle 1. Therefore the offset δ_{13}^e is constant. Also with a similar procedure as was shown for the $l-\psi$ controller, it can be shown that when vehicles 1 and 2 are moving on two parallel straight lines with angles $\theta_{10} = \theta_{20}$ with respect to the x-axis, the orientation of vehicle 3 converges to the following equilibrium trajectory:

$$\theta_3^e = \theta_{10} = \theta_{20} \tag{39}$$

4 Simulation Results

Numerical simulations show the effectiveness of the controller design and the accuracy of the stability analysis. Three simulation examples are presented in this section. In these simulations, the vehicles are assumed to be identical. The controller parameters, λ_1 and λ_2, are selected to be 0.4 for all $l-\psi$ and $l-l$ controllers. The numerical values of the dynamic parameters of the vehicles are as follows [10]:

$$m_{11} = 200\ \mathrm{kg} \qquad m_{22} = 250\ \mathrm{kg}$$
$$m_{33} = 80\ \mathrm{kg.m}^2 \qquad d_{11} = 70\ \mathrm{kg/s}$$
$$d_{22} = 100\ \mathrm{kg/s} \qquad d_{33} = 50\ \mathrm{kg.m}^2/\mathrm{s}$$

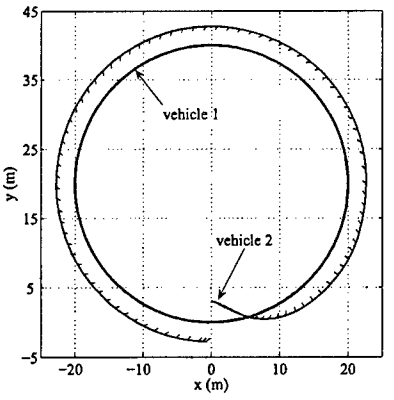

Figure 4: $l - \psi$ Control Circular Motion

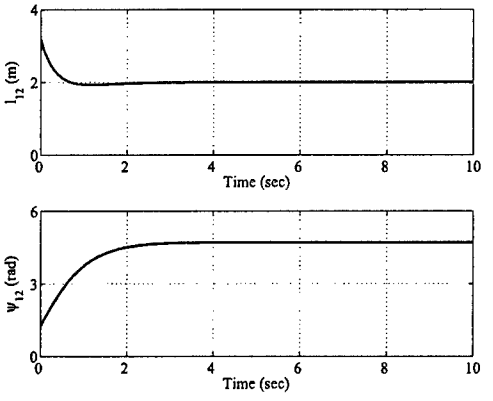

Figure 5: $l - \psi$ Control Parameters

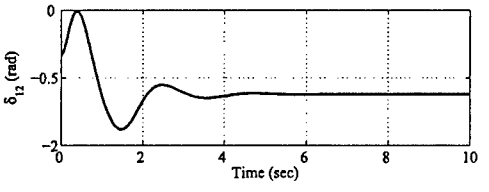

Figure 6: $l - \psi$ Control Orientation Difference

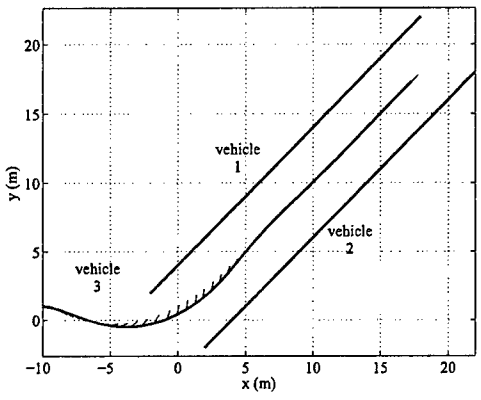

Figure 7: $l - l$ Control Linear Motion

4.1 $l - \psi$ controller

Figure 4 shows two vehicles, where vehicle 2 is commanded to keep a specified distance, $l_{12}^d = 2.0$ meters, and view angle, $\psi_{12}^d = \pi/2$ rad, from vehicle 1. Vehicle 1 is moving on a circle with a radius of 15 m with a constant linear velocity of 9.42 m/s. It is seen that vehicle 2 is far from the specified formation at the beginning of the motion, but it maintains the formation parameters after a while. The orientation of vehicle 2 is shown by the small line segments. Note that due to the dynamics of the vehicle, the orientation is not necessarily tangent to the path, but it is stabilized. The response of the controller outputs, $[l_{12}, \psi_{12}]$, is shown in Fig. 5. As is expected from Eqn. (8), the error dynamics is asymptotically stable and the controller outputs converge to their corresponding desired values asymptotically. Figure 6 shows the difference in the orientation of the two vehicles, δ_{12}. This difference becomes a constant value as dictated by Eqn. (20).

4.2 $l - l$ controller

Three vehicles are shown in Fig. 7. Vehicle 3 is commanded to keep specified distances, $l_{13}^d = 4.0$ and $l_{23}^d = 4.0$ meters, from vehciles 1 and 2, respectively. vehciles 1 and 2 are moving on a straight line at a constant linear velocity of 1.4 m/s. Note that vehcile 3 is not in the specified formation at the beginning of the motion. The figure shows that it maintains the formation parameters after some time. The small line segments show the orientation of vehicle 3. It can be seen that the orientation error is stabilized at zero. The response of the controller outputs, $[l_{13}, l_{23}]$, is shown in Fig. 8. The error dynamics is asymptotically stable, as is expected from Eqn. (31). The difference in the orientation of vehcile 1 and 3, δ_{13}, is shown in Fig. 9. This difference becomes zero as dictated by Eqn. (39).

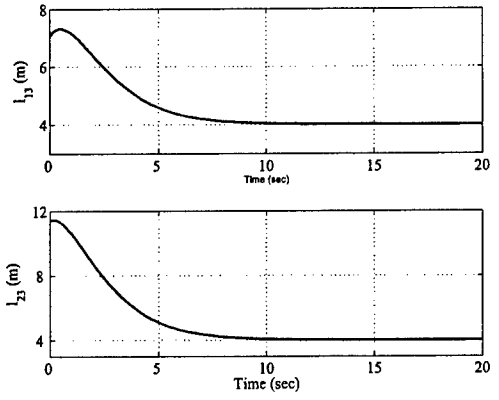

Figure 8: $l - l$ Control Parameters

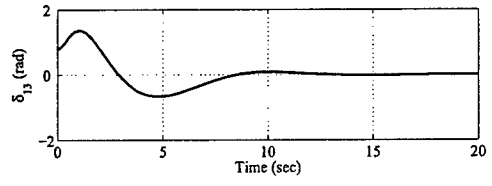

Figure 9: $l - l$ Control Orientation Difference

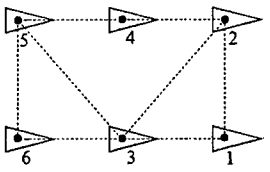

Figure 10: Six Vehilces in a Rectangular Formation

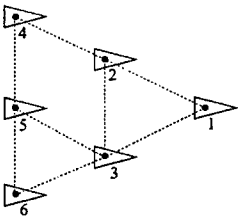

Figure 11: Six Vehicles in a Triangular Formation

Vehicle	Controller	Follows
1	–	a predefined trajectory
2	$l-\psi$	vehicle 1
3	$l-l$	vehicles 1 & 2
4	$l-\psi$	vehicle 2
5	$l-l$	vehicles 3 & 4
6	$l-l$	vehicles 3 & 5

Table 1: Formation Structure Setup

4.3 General formation control

The designed controllers are integrated to control more general formations. This section presents the application of the $l-\psi$ and $l-l$ controllers with multiple vehicles. Figure 10 shows six vehicles that are initially in a rectangular formation. Table 1 summarizes the formation control structure. The same six vehicles are shown in Fig. 11 in a triangular formation. Note that the formation structure that is defined in Table 1 is still applicable for this formation. The only difference between the two formations is the desired values of the formation parameters $[l_{12}^d, \psi_{12}^d]$ and $[l_{13}^d, l_{23}^d]$ for $l-\psi$ and $l-l$ controllers respectively. Two formation change scenarios are presented based on this formation structure.

In the first simulation, it is assumed that vehicle 1 is commanded to move on a parabola by an external trajectory planning algorithm. The group is initially in a rectangular formation similar to Fig. 10, and is commanded to form a triangular formation as shown in Fig. 11. This is equivalent to changing the desired values of the formation parameters. Figure 12 shows the motion of the six vehicles during this maneuver. The vehicles are at their initial positions at lower left corner of the figure. By applying the local controllers, the vehicles successfully change their formation and direction of motion.

In the second simulation, vehicle 1 is moving on a half-sine trajectory that is determined by an external trajectory planning algorithm. The group has a triangular formation as shown in Fig. 11 at the start of the motion. It is assumed that the group has to form a rectangular formation similar to the one shown in Fig. 10. The equivalent desired values of the formation parameters are changed accordingly. The motion of the six vehicles during this maneuver is shown in Fig. 13. Once again the local controllers successfully change the formation of the group.

5 Conclusions

The formation control of an arbitrary number of vehicles was investigated. Two local control laws were introduced that control the relative positions of neighboring vehicles based on sensor information. Since the control schemes are local, each vehicle has to have information about only one or two of its neighbors, depending on the location of the vehicle in the formation. The dynamic models of

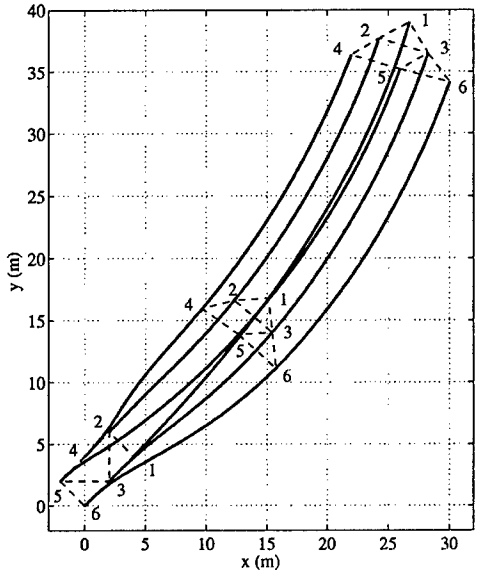

Figure 12: Six Vehicles Changing Formation

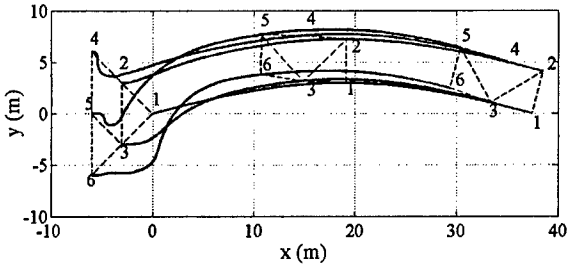

Figure 13: Six Vehicles Changing Formation

the vehicles were used to design the controllers. Since the vehicles are underactuated, the stability of the internal dynamics of the system (orientation of the vehicle) had to be investigated. It was shown that for circular and linear motion of the formation, internal dynamics of the vehicles is asymptotically stable. The effectiveness of the control algorithm was shown by numerical simulations.

Sensitivity to parameter uncertainty, local and global obstacle avoidance, autonomous formation planning, and robustness to failure of a group member are interesting topics that are being investigated. Also, an experimental setup is being designed and built at Center for Nonlinear Dynamics and Control, Villanova University.

References

[1] Yamaguchi, H., 1999. "Cooperative hunting behavior by mobile-robot troops". *International Journal of Robotics Research,* **18**(9), pp. 931–940.

[2] Duman, H., and Hu, H., 2001. "United we stand, divided we fall: Team formation in multiple robot applications". *Journal of Robotic Systems,* **16**(4), pp. 153–161.

[3] Desai, J. P., 2002. "A graph theoretic approach for modeling mobile robot team formations". *International Journal of Robotics and Automation,* **19**(11), pp. 511–525.

[4] Stipanovic, D. M., Inalhan, G., Teo, R., and Tomlin, C. J., 2004. "Decentralized overlapping control of a formation of unmanned aerial vehicles". *Automatica,* **40**(8), pp. 1285–1296.

[5] McDowell, P., Chen, J., and Bourgeois, B., 2002. "UUV teams, control from a biological perspective". In The IEEE Oceans Conference Record, Vol. **1**, pp. 331–337.

[6] Martins, A., Almeida, J. M., and Silva, E., 2003. "Coordinated maneuver for gradient search using multiple AUVs". In The IEEE Oceans Conference Record, Vol. **1**, pp. 347–352.

[7] Ihue, I. F., Skjetne, R., and Fossen, T. I., 2004. "Nonlinear formation control of marine craft with experimental results". In Proceedings of the IEEE Conference on Decision and Control, Vol. **1**, pp. 680–685.

[8] Fossen, T. I., 1994. *Guidance and Control of Ocean Vehicles.* John Wiley & Sons.

[9] Fahimi, F., Nataraj, C., and Ashrafiuon, H., 2004. Real time obstacle avoidance for groups of mobile robots. Submitted to Journal of Robotic Systems for possible publication.

[10] Rayhanoglu, M., 1997. "Exponential stabilization of an underactuated autonomous surface vessel". *Automatica,* **33**(6), pp. 2249–2254.

REPORT DOCUMENTATION PAGE

Form Approved
OMB No. 0704-0188

1. REPORT DATE *(DD-MM-YYYY)*	2. REPORT TYPE	3. DATES COVERED *(From - To)*
22-08-2005	Final Technical Report	June 1, 2004 - May 31, 2005

4. TITLE AND SUBTITLE
Real Time Trajectory Planning for Groups of Unmanned Vehicles

5a. CONTRACT NUMBER

5b. GRANT NUMBER
N00014-04-1-0637

5c. PROGRAM ELEMENT NUMBER
04PR11370-00

6. AUTHOR(S)
Farbod Fahimi

5d. PROJECT NUMBER

5e. TASK NUMBER

5f. WORK UNIT NUMBER

7. PERFORMING ORGANIZATION NAME(S) AND ADDRESS(ES)
Center for Nonlinear and Control, Department of Mechanical Engineering, Villanova University, 800 Lancaster Ave., Villanova, PA 19085, USA

8. PERFORMING ORGANIZATION REPORT NUMBER
N/A

9. SPONSORING/MONITORING AGENCY NAME(S) AND ADDRESS(ES)

10. SPONSOR/MONITOR'S ACRONYM(S)

11. SPONSOR/MONITOR'S REPORT NUMBER(S)

12. DISTRIBUTION/AVAILABILITY STATEMENT
Approved for public release; distribution is Unlimited.

13. SUPPLEMENTARY NOTES

14. ABSTRACT

Feedback control laws for controlling multiple unmanned surface vehicles in arbitrary formations are proposed. The presented formation control method uses only local sensor-based information. The method of input-output linearization is used to exponentially stabilize the relative distance and orientation of neighboring vehicles with a three-degree-of-freedom dynamic model. It is shown that the internal dynamics of the system is also stable. The use of these control laws are demonstrated by computer simulations. These controllers can be utilized to control the an arbitrary large number of unmanned surface vehicles in very general formations.

15. SUBJECT TERMS
Unmanned surface vehicles, Formation Control, Decentralized control, Input-output linearization

16. SECURITY CLASSIFICATION OF:			17. LIMITATION OF ABSTRACT	18. NUMBER OF PAGES	19a. NAME OF RESPONSIBLE PERSON
a. REPORT	b. ABSTRACT	c. THIS PAGE			Farbod Fahimi
UU	UU	UU	SAR	17	19b. TELEPHONE NUMBER *(Include area code)* 610 519 4949